DEVELOPMENT OF A SCIENTIFIC PERMANENT SCATTERER SYSTEM: MODIFICATIONS FOR MIXED ERS/ENVISAT TIME SERIES

Nico Adam, Bert Kampes, Michael Eineder

German Aerospace Center Oberpfaffenhofen, 82234 Wessling (Germany), Nico.Adam@dlr.de

ABSTRACT

The permanent scatterer technique invented at POLIMI has meanwhile developed into a remarkable operational method. It facilitates innovative data products such as urban subsidence maps or atmospheric delay measurements and permits new geophysical applications. The accuracy and validity of this techniques has been demonstrated in several projects at DLR. Due to the outstanding availability of data, time series of this technique have mainly been produced from data of the compatible satellite sensors ERS-1 and ERS-2. These time series can even span a continuous time range of about twelve years. This long-term observation enables the monitoring of displacements with millimetre accuracy and even facilitates the detection of seasonal periodic effects.

The sensor ERS-1 made its last acquisition in 2000. The similarly constructed successor ERS-2 still monitors the Earth's surface even after nine years of operation. But recent acquisitions are unfortunately not suited for general interferometric applications. The reason is a heavily varying Doppler centroid frequency due to failures of gyros. The ERS-2 successor ENVISAT/ASAR is able to pursue the unique continuity in the monitoring of urban areas. But it operates with a slightly different radar frequency compared to the ERS sensors. Consequently the interferometric principle becomes more complicated and the processing has to be modified. We will present the required changes for the permanent scatterer cross interferometry on the developed scientific permanent scatterer system.

1. INTRODUCTION

The permanent scatterer (PS) technique utilizes a single master stack of interferograms and restricts the parameter estimation for velocity and DEM update on particular long time stable scatterers [1]. The estimation is based on the three dimensions baseline, time difference and scatterer location. The dimension time is added to the conventional InSAR technique using only two acquisitions. I.e. time series analysis is possible and the range line effects atmosphere, orbit error and displacement can be separated. Consequently, displacement can be monitored with millimeter accuracy.

Rocca showed in [2] that variability of the available baselines and a large number of scenes improve the precision of the estimated parameters. In order to firstly guarantee the continuity in the subsidence monitoring and secondly to increase the number of available scenes as well as the variability of the available baselines data of the sensors ERS and ENVISAT can be coherently combined. Alternatively to the permanent scatterer cross interferometry two independent time series can be generated, one for ERS and one for ENVISAT which can be fused afterwards. Both techniques already have been described in [3], [4] and in [5]. DLR's PS system was adapted for the cross interferometry and tested with data from the test sites Las Vegas and Paris. For the city of Las Vegas 46 ERS and 8 ENVISAT scenes area available whereas for the city of Paris 100 ERS and 10 ASAR scenes are available.

The next section briefly describes the cross InSAR theory. Afterwards the major PS system modifications such as the PS detection are explained theoretically in section 3, practically in section 4. Section 5 reports about the cross InSAR PS survival rate which is the criterion for the choice for one of the two fusion methods. Section 6 elaborates on the PS estimation.

2. CROSS-INSAR THEORY

The slightly different wavelengths of the sensors ERS and ENVISAT/ASAR have a major impact on the InSAR principle. Conventional interferometry measures the phase

$$\varphi = \frac{4 \cdot \pi}{\lambda}\left(R_1 - R_2\right) \tag{1}$$

R_1 and R_2 are the range distances between the respective sensor and the observed point and λ is the radar wavelength. A phase pattern which depends on the effective baseline B_{eff} results which enables the measurement of the topography, provided that $B_{eff} \neq 0$. Utilized is the look angle dependency of the observed phase. Fig. 1 visualizes the interferometric phase

Proc. of the 2004 Envisat & ERS Symposium, Salzburg, Austria
6-10 September 2004 (ESA SP-572, April 2005)

patterns for an effective baseline of 200 m and 600 m showing the increasing height sensitivity with larger baselines.

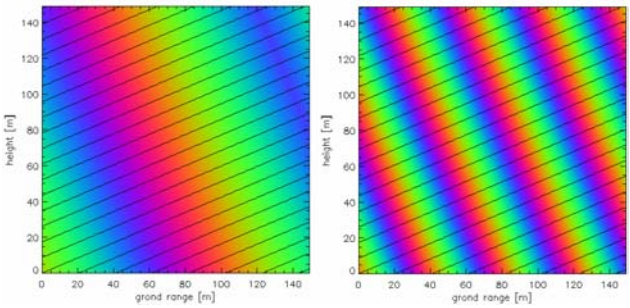

Fig. 1: Conventional single wavelength InSAR phase pattern for B_{eff}=200m (left) and B_{eff}=600m (right); black lines are iso-range lines.

With two different wavelengths λ_1, λ_2, the interferometric phase pattern is composed of two contributions. Firstly, the conventional interferometry phase term remains. Secondly, a range distance dependent phase pattern is superimposed. This latter term contains no information about the look angle.

$$\varphi = \frac{4\cdot\pi}{\lambda_2}\cdot(R_1 - R_2) + \frac{4\cdot\pi\cdot(\lambda_2-\lambda_1)}{\lambda_1\cdot\lambda_2}\cdot R_1 \qquad (2)$$

Eq. 2 has been reported in [3] and in [5] as well. It shows that in the case of cross interferometry the precise range of a scatterer needs to be considered in the estimation of the parameters using cross interferograms. Fig. 2 visualizes the resulting fringe patterns for effective baselines of 0m and 1200m. For the zero baseline the conventional term equals zero, thus the fringe pattern is caused only by the range dependent term. One phase cycle (2π) is related to 4.84 m along the line of sight in the case of ERS and ENVISAT/ASAR.

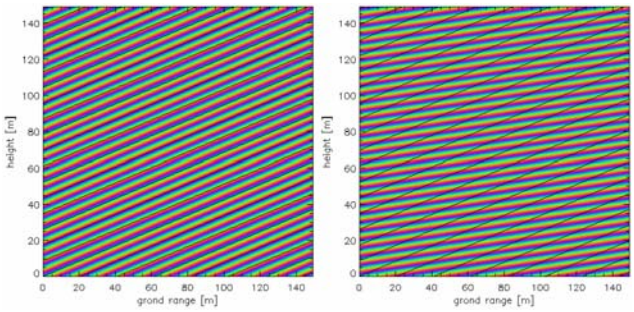

Fig. 2: Cross InSAR phase pattern for B_{eff}=0m and B_{eff}=1200m. A phase pattern is visible also for the zero baseline situation, caused by the different wavelengths.

3. PS DETECTION THEORY

In the permanent scatterer interferometry, the processsing is restricted to long term stable scatterers. Therefore, these stable objects need to be detected in the radar scenes. In this section, two methods are described and compared that can be used to detect these scatterers. The first procedure is the Signal to Clutter Ratio (SCR) method [6]. And the second technique is called the Dispersion Index method [1]. It will be shown that both techniques are based on one and the same signal model. This is the starting point to derive the properties of both detectors which are actually estimators for the SCR and consequently for the phase error of the point scatterer observation. The advantages and disadvantages of both methods are explained. Finally, the practical realization of the PS detection in the PS cross interferometry system is described because it is the basis to check for the phase continuity of point scatterers in the cross interferometry in a given stack of mixed radar scenes.

Assuming decorrelated clutter and neglecting thermal noise the phase error ϕ of a point scatterer observation is determined by its SCR. This is confirmed by the equation for the probability density function (pdf) for the phase error of a point scatterer observation:

$$pdf(\varphi) = \frac{\sqrt{SCR}\cdot|\cos(\varphi)|}{\sqrt{\pi}}\cdot e^{-SCR\cdot\sin^2(\varphi)} \qquad (3)$$

Fig. 3 shows the phase probability density function for different SCRs. This figure illustrates that a high SCR corresponds to a small phase error whereas with a decreasing SCR the phase error increases. Therefore, the PS can be detected by the point scatterers with a high SCR.

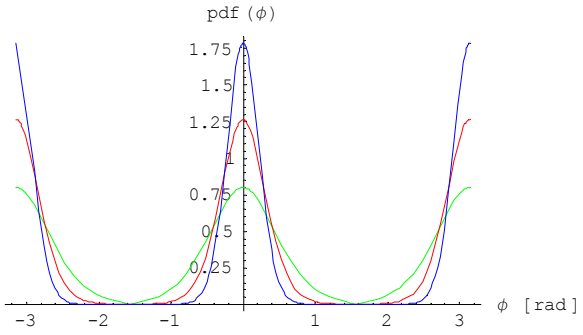

Fig. 3: Phase error probability density function of a point scatterer observation depending on the SCR (high and narrow curve (blue): SCR=10; lower and wide function (red): SCR=5; lowest curve (green): SCR=2).

Eq. 3 is a valid pdf- approximation for SCR better than three and it is still usable for SCRs of about two. It can only describe the probability in the phase range –π/2 .. +π/2. Therefore, the exact phase error pdf for a point scatterer observation was derived as well:

$$pdf(\varphi) = \tag{4}$$

$$\frac{e^{-\mathrm{SCR}}\left(2\sqrt{\pi}\,\sqrt{\mathrm{SCR}}\,\cos(\phi)\left(\sqrt{\sec^2(\phi)}\,\cos(\phi)+\mathrm{erf}\left(\sqrt{\mathrm{SCR}}\,\cos(\phi)\right)\right)\left(\cosh(\mathrm{SCR}\,\cos^2(\phi))+\sinh(\mathrm{SCR}\,\cos^2(\phi))+2\right)\right)}{4\pi}, \quad |\varphi| < \pi/2$$

$$-\frac{e^{-\mathrm{SCR}}\left(e^{\mathrm{SCR}\cos^2(\phi)}\sqrt{\pi}\,\sqrt{\mathrm{SCR}}\,\cos(\phi)\left(\mathrm{erfc}\left(\sqrt{\mathrm{SCR}}\,\cos(\phi)\right)+\mathrm{sgn}(\cos(\phi))-1\right)-1\right)}{2\pi}, \quad |\varphi| \geq \pi/2$$

Fig. 4 demonstrates that Eq. 4 correctly describes the full phase range $-\pi \ldots +\pi$. Especially, with a $SCR \rightarrow 0$ the pdf moves towards the uniform density.

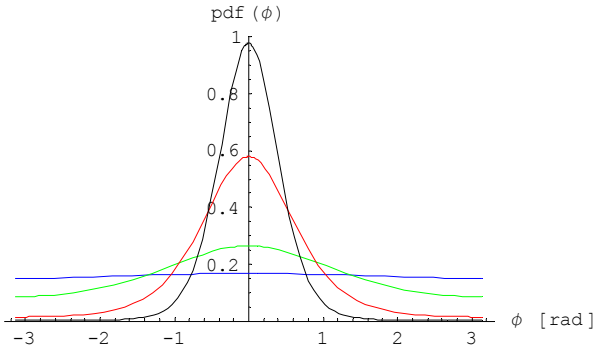

Fig. 4: Exact phase error pdf of a point scatterer observation depending on the SCR black: SCR=3; red: SCR=1; green: SCR=1; blue: SCR=0.001.

Two different methods are known to estimate the SCR. Firstly, the Signal to Clutter Ratio (SCR) method [6] that estimates the clutter from neighbouring pixels and secondly the Dispersion Index method [1] that infers the Clutter from the amplitude dispersion of the resolution cell containing the PS. The SCR method was presented on the SAR Calibration workshop in ESTEC in 1993. It was developed to check the phase stability of corner reflectors (CRs). This technique requires a spatial estimation window around the point scatterer. With CRs surrounded only by clutter there is no problem to fulfil this requirement. But with real permanent scatterers which are often in the neighbourhood of other man-made objects this estimation window can introduce some nuisances. The SCR method is a two-step procedure: firstly the point scatterers need to be detected and in a second step the SCR is estimated for the detected point scatterer. The Dispersion Index method was directly developed for the PS technique. The Dispersion Index D_A is the ratio of the amplitude's standard deviation σ_A and of the mean amplitude m_A.

$$D_A = \frac{\sigma_A}{m_A} = f(SCR) = \frac{1}{\sqrt{2 \cdot SCR}} \tag{5}$$

Ferretti already showed in [1] by simulation that there is a relation between the dispersion index D_A and the phase error in the permanent scatterer observation. In the following the signal model for both estimators is explained.

A dominant scatterer is spatially surrounded by incoherent clutter. The observed phase measurement of a resolution cell is therefore composed of a dominant signal and a superposition of the clutter. The phase of the main scatterer is related to the range distance of the scatterer to the sensor but the resulting phase caused by the clutter is random. Depending on the ratio of the signal to the clutter power the phase error ϕ varies. The resulting signal composition for the effective values (RMS) of the signal s and the clutter c and the resulting mean phase error σ_ϕ is shown in Fig. 5.

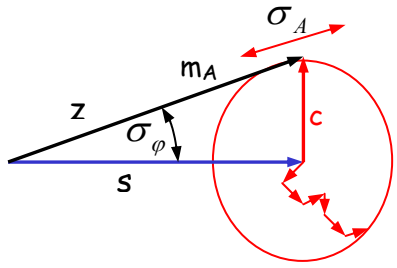

Fig. 5: Signal model for a point scatterer observation.

The SCR method estimates the length of the vectors s and c (Fig. 5) of a point scatterer by a point target analysis. The assumption is that the clutter inside the resolution cell is the same as in the surrounding resolution cells. Therefore a spatial estimation window is required. The effective phase error can be estimated by:

$$\varphi_{err}^{SCR} = \frac{1}{\sqrt{2 \cdot SCR}} \tag{6}$$

Contrarily, the Dispersion Index method estimates the mean amplitude m_A and the amplitude's dispersion σ_A over time. Corresponding to Fig. 5, the following equation represents the estimate for the mean phase error:

$$\varphi_{err}^{D_A} = \arctan\left(\frac{m_A}{\sigma_A}\right) \quad (7)$$

and can be approximated for small phase error values by:

$$\varphi_{err}^{D_A} \approx \frac{m_A}{\sigma_A} \quad (8)$$

Because the SCR and the Dispersion Index method are both estimators for the expected phase error based on the SCR, their properties are described and compared in the following. The SCR method needs a spatial estimation window and consequently its spatial resolution is limited. Advantageously, this estimator results in an estimate for the SCR of a point scatterer in each radar scene of a data stack. Consequently, it can track the evolution of the SCR over time. The Dispersion Index method is based on the time series analysis of the scatterer's amplitude. Consequently, no spatial estimation window is involved into the estimation procedure. And therefore the SCR can be estimated with the full radar resolution. A drawback is the single SCR measurement for the whole time series which actually represents the expected temporal SCR of a point scatterer. In other words, the temporal resolution of this method is limited and requires the calibration of each scene.

In order to determine the properties of both estimators a simulation was carried out. Fig. 6 visualizes the result. Both estimators are biased. The bias increases with decreasing SCR. Compared to the SCR method the Dispersion Index method is more optimistic (i.e. biased) about the phase error of a point scatterer. But knowing this behaviour, the estimation can be improved (yet not full corrected) concerning this bias. The variance of the estimated value depends for the Dispersion Index method on the number of the available temporal samples. The more temporal samples are available the more the estimation variance is reduced. Fig. 7 and Fig. 8 visualize this relation. For Fig. 7 a point scatterer with a SCR of eight whereas for Fig. 8 a SCR of two are simulated. The black line corresponds to the true expected phase error. The green line is the biased temporal mean phase error estimate of the Dispersion Index method. And the dotted green lines describe the standard deviation of the estimate as it varies around the mean (green line). The variance for the high SCR (Fig. 7) is compared to the low SCR (Fig. 8) much smaller. I.e. the SCR influences the variance of the estimate. Obviously, the dispersion increases with decreasing SCR. Fig. 7 and Fig. 8 show that with more than 20 radar scenes the estimation variance remains nearly constant. Consequently, 20 radar scenes are sufficient in order to receive an estimate for the expected temporal phase error of a point scatterer. On the contrary, if the number of available radar scenes is less this phase error can not be predicted with good confidence.

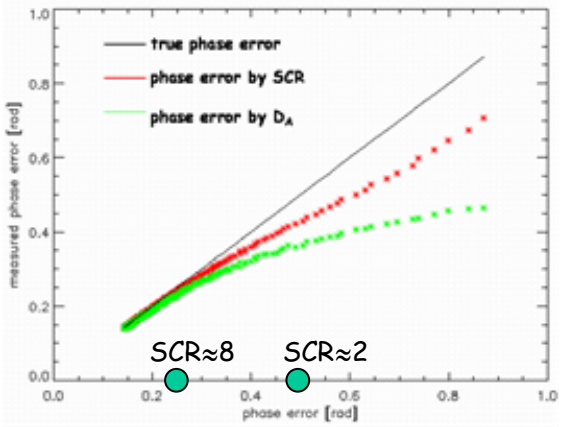

Fig. 6: Estimation bias for the expected phase error of the SCR and the Dispersion Index method.

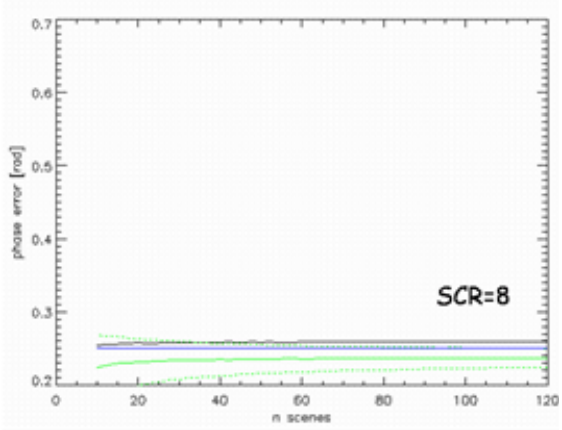

Fig. 7: SCR=8 bias and variance of the Dispersion Index method depending on the number of available temporal samples (radar scenes).

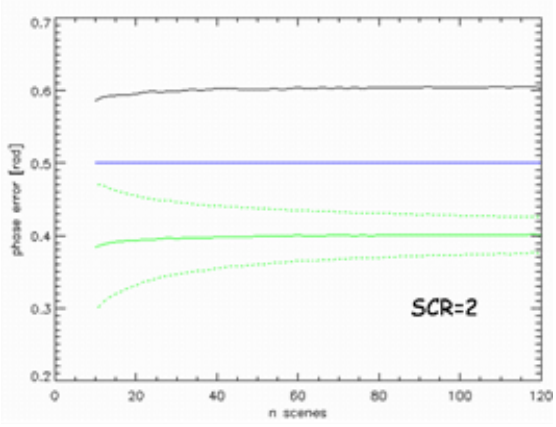

Fig. 8: SCR=2 bias and variance of the Dispersion Index method depending on the number of available temporal samples (radar scenes).

4. PS DETECTION REALISATION

With radar cross interferometry, additional effort is required to check if the PS candidate is phase stable within the ERS data and the ENVISAT data. Therefore, a new PS detection algorithm was developed. Because two different radars are used the PSs should be detected in the respective time series exclusively. The intersection of both independent PS sets can be used for the joined estimation. At the moment only ten ENVISAT scenes are available. It was shown before that the Dispersion Index method requires more than 20 scenes in order to reliably estimate the mean temporal phase error, respectively the SCR. Consequently, the detection of the PS in the ENVISAT time series can only be achieved by the SCR method. The drawbacks of this method were described above. A spatial estimation window and the fact that the clutter is estimated from the surrounding resolution cells can cause misinterpretations with this method. Therefore with such a simple method it can be expected that the PS-density for the cross interferometry is underestimated.

Nevertheless, the following examples are provided to give an impression about this matter. The point scatterers in the data stack's scenes are firstly detected and secondly their SCR is estimated. The detection of the point scatterers showed up with a nearly identical scatterer density for both sensors as is visible in Fig. 9. The small PS density indicates that not all point scatterers were detected.

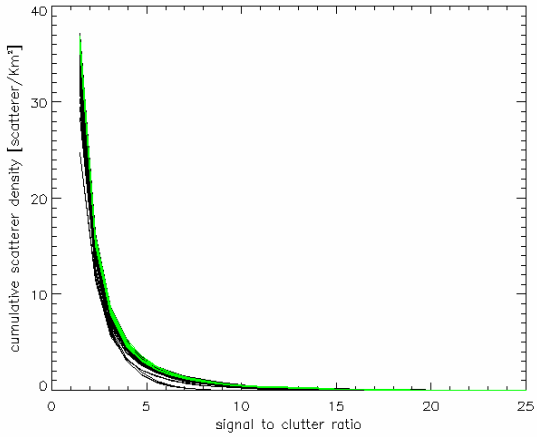

Fig. 9: Point scatterer density obtained in the Paris test site with a simple SCR detection. black: ERS green: ENVISAT/ASAR.

Fig. 11–14 show examples for detected PS in the Paris test area. The detection differs not only between the sensors ERS and ENVISAT but also between the acquisitions with one and the same sensor. Highlighted are only PS with a SCR better than 2. Fig. 15 presents the detection of PS via the preceding method from the ERS data. Obviously, a better PS density can be obtained using this method. In Fig. 15 the quality of the PS is coded by colour. The phase stability improves starting with green, passing yellow and the best indicates the red colour. Because the detected PS are too different and the PS density is not in the usual range this simple SCR technique can not be applied. Instead the point scatterers are detected from the reflectivity mean map of the ERS ENVISAT joint time series. Of course they are mainly detected due to the ERS data. The assumption is that the detected ERS point scatterers are all candidates for the ENVISAT time series. This procedure guarantees the detection of PS with the usual density as can be seen in Fig. 16. The final average PS density is about 120 PS/km^2 for the Paris and Las Vegas test site. But in the city center of Paris up to 300 PS/km^2 are detected.

The detected point scatterers form the basis for the following precise SCR analysis applying Eq. 6. The result is an expected phase error estimate for each point scatterer in each radar scene. Consequently, the temporal evolution over time can be plotted. Fig. 10 gives an example of this procedure.

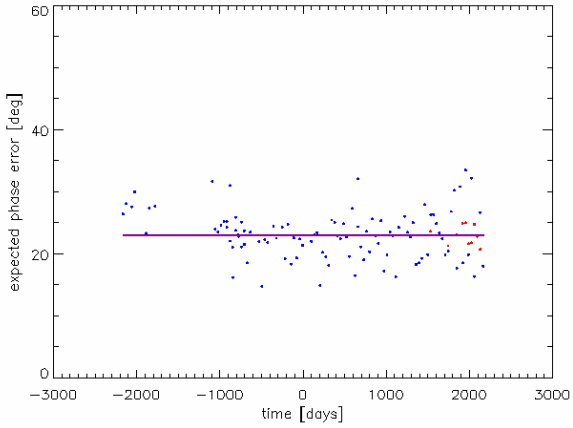

Fig. 10: Estimated evolution in time of the phase error of the PS.

Two different groups of measurements are available. One group results from the ERS sensors whereas the other group was generated from the ENVISAT data. The independent group measurements are highlighted with blue for ERS and red colour for the ENVISAT data in the figures. The subject of the assessment is to detect the PS with a phase continuity between the sensors ERS and ENVISAT. Consequently the decision is to be made whether the temporal mean phase error of the ENVISAT data is the same or even better than the expected phase error of the ERS time series. If this is the case then a cross interferometry permanent scatterer is detected. On the contrary, if the temporal mean phase error of the ENVISAT data is worse then the PS is not suited for cross interferometry (Fig. 17). This means that the problem of comparing two independent time series needs to be solved. This is realized by the Mann-Whitney test and the one-sample median test (Wilcoxon test). From Fig. 18 it is obvious that the f_{DC}

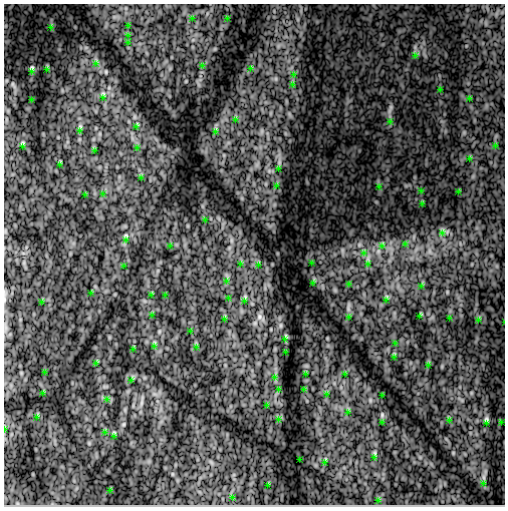

Fig. 11: ENVISAT/ASAR scene with selected PS (orbit 1522 test site Paris).

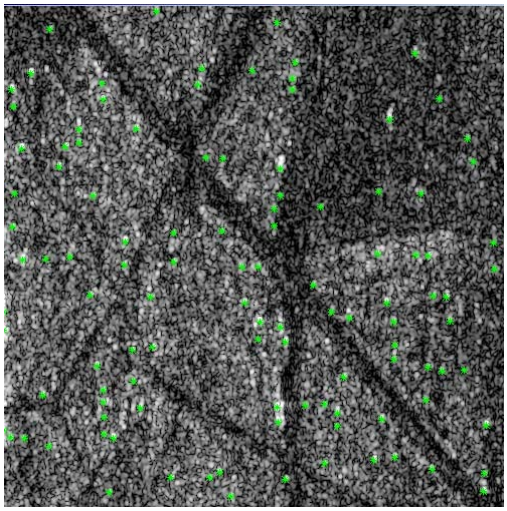

Fig. 12: ERS-2 scene with selected PS (orbit 39398).

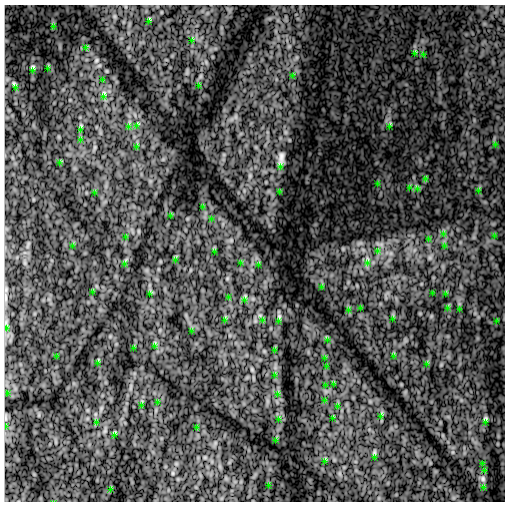

Fig. 13: ERS-2 scene with selected PS (orbit 10340).

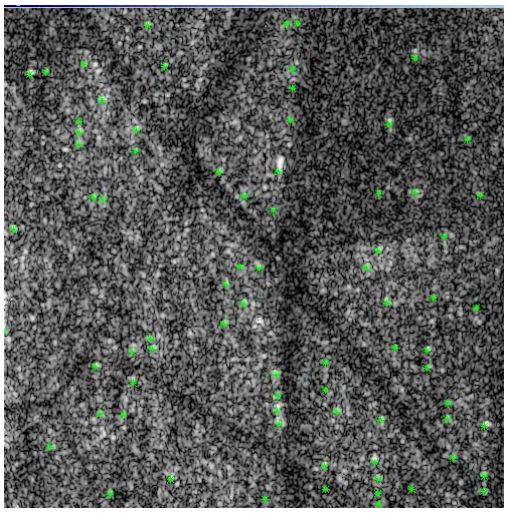

Fig. 14: ERS-1 scene with selected PS (orbit 4619).^

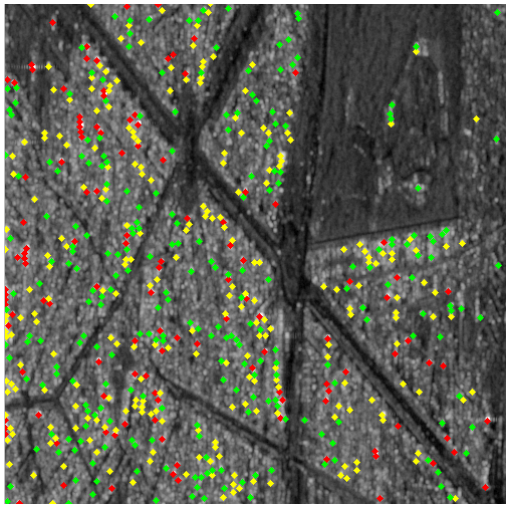

Fig. 15: ERS time series based PS detection; green: 70% yellow: 80% red 90% of the scenes above the RCS threshold (preceding method).

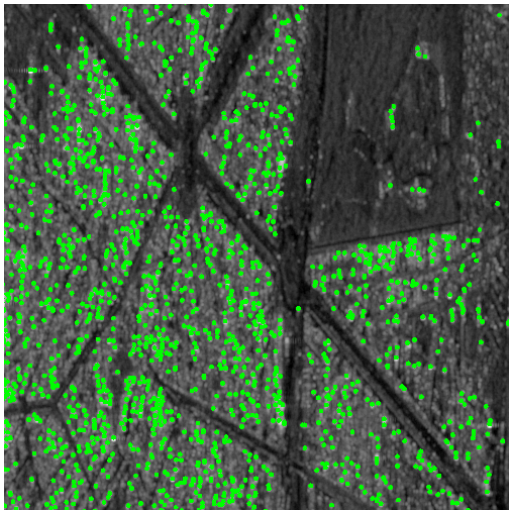

Fig. 16: Detected PS in the mean reflectivity map of the ERS ENVISAT/ASAR joint time series.

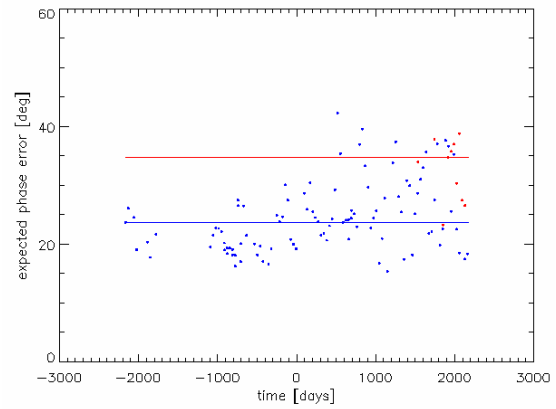

Fig. 17: Evolution in time of the phase error for a non-optimal PS.

deviation of the sensor ERS-2 can introduce noticeable SCR estimation deviations in practice. Because of the small sample size and the possibility of outliers the median is applied during the practical assessment of the data. The two statistical tests are for

$$\tilde{\varphi}_{err}^{ERS} \geq \tilde{\varphi}_{err}^{ENVISAT/ASAR} \qquad (9)$$

and consequently both need to be adapted. The two test procedures are implemented and were compared resulting in similar results as will be shown in the next section.

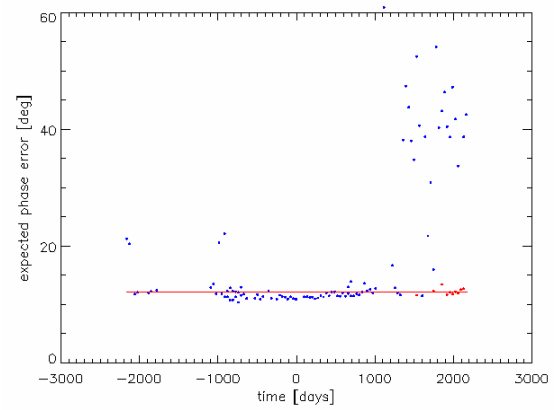

Fig. 18: The robust Median estimator helps to decrease misinterpretation.

5. PS CONTINUTIY

An important question in the cross interferometry is whether the sensors ERS and ENVISAT/ASAR observe one and the same point scatterer and if these are working as permanent scatterers. The subject is not only to show the availability of cross interferometry permanent scatterers but also to estimate the amount of PS which survive in the ENVISAT/ASAR time series. This information influences the choice for one of the two processing options. In case the PS survival rate is low the fusion of the two independent time series estimations is optimal because the PS density is increased in that case. Cross interferometry estimation is to be preferred in case of a high survival rate of the PS for reasons of improved estimation accuracy.

The PS survival assessment turns out to be difficult due to the small number of available ENVISAT/ASAR scenes. But the implemented PS detection provides this information based on the amplitude information only. The statistical tests described in the previous section are applied on the data of the Paris and the Las Vegas test site.

For Paris about 52000 point scatterers are detected and considered to be cross interferometry PS candidates. With a confidence level of 95% ca. 2600 PS can be misdetected. In the data of the test site Las Vegas nearly 306000 permanent scatterer candidates were detected and analyzed.

The green color in Tab. 1 and Tab. 2 indicates the survived PS of the ERS in the ENVISAT/ASAR time series. Contrarily, the red depicts the PS that did not survive. The reason for the phase discontinuity can be a temporal change of the scatterer. But this effect should not be the major one. Instead the unsuitable look angles in range and azimuth are assumed to be the reason. The look angles are parameterized by the effective baseline and the Doppler centroid frequency f_{DC}. If the baseline for an ERS- ENVISAT/ASAR cross interferogram is in the range of ca. 2300m ±1200m then all point scatters should be coherent in the phase image because even distributed scatterers can be coherently observed with such a baseline configuration. The formed baselines in the generated InSAR stacks of Paris and Las Vegas are far away from this optimal baseline range. In contrast, the ENVISAT/ASAR Doppler centroid frequency f_{DC} deviates only a little and is still close to the ERS f_{DC}. Therefore the PS survival results mainly from the scatterer size respectively its shape and the baseline configuration. Tab. 1 lists the result from the Mann-Whitney test and Tab. 2 from the one-sample median test.

Tab. 1: Number of point scatters belonging to different types applying the Mann-Whitney test: green colour is related to a survived PS; red corresponds to phase discontinuity.

test site:	Paris	Las Vegas
$\varphi_{err}^{ENVISAT/ASAR} < \varphi_{err}^{ERS}$	8991 (17%)	40503 (13%)
$\varphi_{err}^{ENVISAT/ASAR} = \varphi_{err}^{ERS}$	34893 (66%)	205411 (67%)
$\varphi_{err}^{ENVISAT/ASAR} > \varphi_{err}^{ERS}$	8906 (17%)	59991 (20%)

Tab. 2: Number of point scatters belonging to different types applying the one-sample median test

test site:	Paris	Las Vegas
$\varphi_{err}^{ENVISAT/ASAR} < \varphi_{err}^{ERS}$	7925 (15%)	30028 (10%)
$\varphi_{err}^{ENVISAT/ASAR} = \varphi_{err}^{ERS}$	37021 (70%)	232846 (76%)
$\varphi_{err}^{ENVISAT/ASAR} > \varphi_{err}^{ERS}$	7844 (15%)	43031 (14%)

Comparing the PS survival rates in the Tab. 1 and Tab. 2 it becomes visible that the test procedures decide differently strict for equality of the temporal mean phase error. Fig. 19 and Fig. 20 show examples for the different detection behaviour. In both cases a misdetection can not really be noticed and therefore the observed behaviour is not a problem. The two test procedures show up with similar results for the cross interferometry PS survival rate. If 5% misdetection can be tolerated then about 80% - 85% of the scatterers are available in the ERS time series as well as in the ENVISAT/ASAR time series.

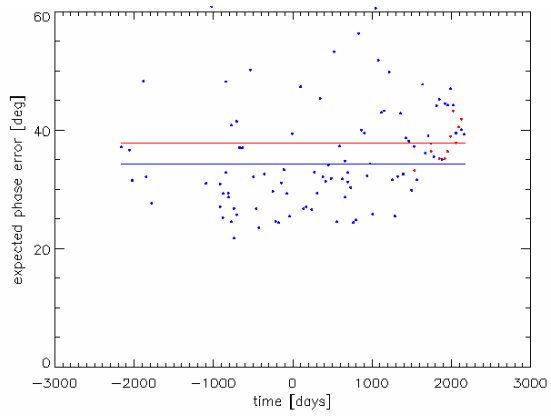

Fig. 19: The Mann-Whitney test detects an equal phase error but the one-sample median test detects a phase discontinuity.

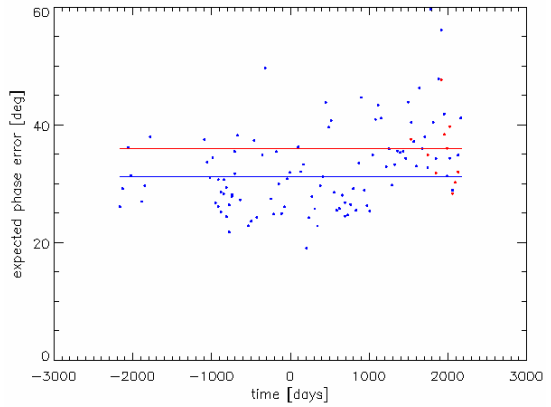

Fig. 20: Contrary to Fig. 19, the Mann-Whitney test detects a phase discontinuity but with the one-sample median test an equal temporal mean phase error is identified.

6. PS ESTIMATION

The ERS and the ENVISAT/ASAR data can be fused applying two methods. Firstly, the data can coherently be combined forming cross interferograms. Secondly, the parameter estimates of individual time series are joined.

With the cross interferograms the precise information about the slant range position is introduced into the phase measurement (Eq. 2). This position is fixed by the master scene and each PS has it's own position. Consequently, the position dependent phase needs to be estimated for each PS respectively for each relative estimation PS pair. It can be estimated as a phase offset between the phase values of the ERS and the ENVISAT/ASAR scenes. I.e. the offset is the same for all cross interferograms in a single PS estimation. Unfortunately, this offset phase cannot be integrated into an absolute PS position as the displacement or the DEM update. The reason is the range position phase ambiguity of ca. 5 m whereas the pixel spacing is about 8 m. Therefore, the estimation procedure was modified. At the arcs of the PS estimation network, the relative parameters (difference in DEM error, difference in displacement rate, difference in azimuth position and cross interferometry phase offset) using the integer least-squares estimator are estimated. This algorithm takes the properly propagated variance-covariance matrix into account, and uses the estimated precision of the phase observation for correct weighting of the data, also see [7]. The residual phase at the PS is obtained for each interferogram by least-squares integration of the residuals at the arcs of the network. For each interferogram a low-pass phase screen is computed by spatially filtering these residual fields (which are composed of atmospheric signal, un-modeled displacement, and random noise). All interferograms are corrected for the computed low-pass phase screens, which enables a direct point-by-point estimation of the parameters. This estimation can be regarded as a temporal phase unwrapping with the help of a displacement model. The unwrapped model phase at each PS can be computed using the estimated parameters, and the phase data at the PS positions can be unwrapped by adding the low-pass phase screens. After this step, a final parameter estimation is performed through the unwrapped data. Fig. 2 and Fig. 23 visualize the estimated displacement rates using cross interferograms for the two test sites.

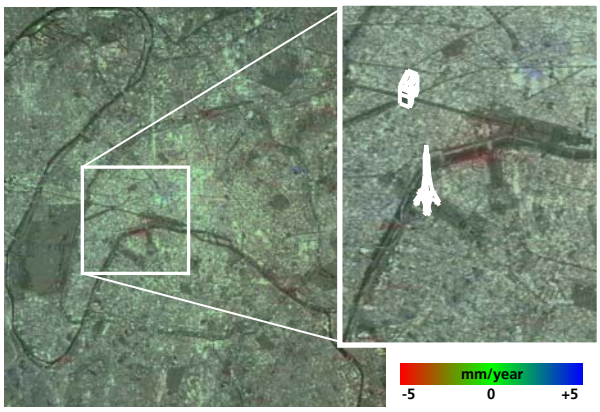

Fig. 22: Subsidence estimation for city of Paris including ten cross interferograms.

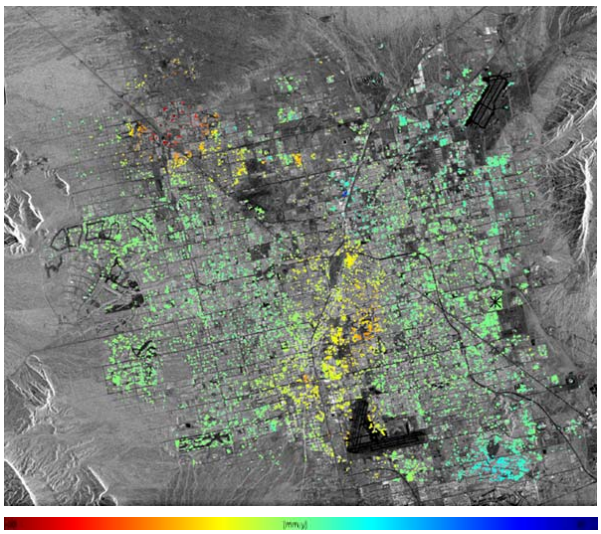
Fig. 23: Estimation of linear displacement rates for the city of Las Vegas including eight cross interferograms.

The alternative estimation method i.e. the fusion of the independent time series is considered ineffective at the moment. The small amount of ENVISAT/ASAR data requires to restrict the estimation for this time series in order to cope with the phase ambiguities. It can be expected that the overall PS density will increase by about 15% - 20%. But the resulting precision can not really be compared with the one obtained from the long ERS time series.

7. CONCLUSION

DLR's PS processor has been successfully adapted for cross interferometry. The most promising method i.e. the coherent combination has been implemented. The reason is the expected improved estimation accuracy due to the increased number of scenes and the better variability of the baselines.

Due to the non-optimal baseline configurations in the test sites it was expected that not all point scatterers remain phase stable regarding the ERS observation. In order to assess this effect the SCR was used as an indicator for the phase stability. The SCR can be estimated directly from the radar data utilizing the intensity information only. With standard statistical methods the amount of permanent scatterers which survive in the ENVISAT/ASAR time series was estimated. About 80% - 85% of the point scatterers can be considered to be usable for the cross interferometry. This assessment confirms that the cross interferometry between ERS and ENVISAT/ASAR is a useful method to continuously monitor subsidence effects in urban areas.

Moreover, the cross interferometry can even be used to increase the PS density. Because the PS amount is nearly the same in the radar scenes of the different sensors the lost 15% - 20% of point scatterers can be used in an independent ENVISAT/ASAR time series alone. Only the number of available scenes in the ENVISAT/ASAR time series needs to be higher for that reason.

8. ACKNOWLEDGMENT

The authors would like to thank ESA for supplying the ERS and ENVISAT/ASAR data in the course of the project 16702/02/I-LG.

9. REFERENCES

1. Ferretti A., C. Prati, F. Rocca, 'Permanent Scatterers in SAR Interferometry'. *TGARS*, Vol. 39, No. 1, pages 8-20, January 2001.

2. Rocca F., 'Diameters of the Orbital Tubes in Long-Term Interferometric SAR Surveys'. *TGARS*, pages 1-4, 2004.

3. Arrigoni M., C. Colesanti, A. Ferretti, D. Perissin, C. Prati, F. Rocca, 'Identification of the Location Phase Screen of ERS-ENVISAT Permanent Scatterers', http://earth.esa.int/workshops/fringe03/participants/546/paper_proceedings_ers_envi_ps1.pdf, *FRINGE* 2003.

4. Colesanti, A. Ferretti, R. Locatelli, G. Savio. 'Multi-platform permanent scatterers analysis: first results'. *Second GRSS/ISPRS Joint Workshop,* Berlin, pages 52-56, 2003.

5. Colesanti C., A. Ferretti, C. Prati, D. Perissin, F. Rocca, 'ERS-ENVISAT Permanent Scatterer interferometry' In *IGARSS*, Toulouse, 2003.

6. *CEOS SAR Calibration Workshop*, ESTEC, Noordwijk, Netherlands, September 1993.

7. Kampes, B.M., R.F. Hanssen, 'Ambiguity resolution for Permanent Scatterer Interferometry'. Accepted for publication in TGARS, 2004.